# Mode-locking with ultra-low intra-cavity pulse intensity using enhanced Kerr nonlinearity

Mallachi Elia Meller, Shai Yefet and Avi Pe'er, *Member, OSA,*

***Abstract*—Kerr lens mode locking strongly depends upon intensity. Low pulse intensity weakens the nonlinear Kerr lens, and eventually mode locking is not supported. We demonstrate efficient mode-locking in a Ti:Sapphire laser oscillator with record-low intra-cavity pulse intensity (18 GW/cm$^2$) and intra-cavity average power (340 mW). Using an additional nonlinear window in the cavity, the Kerr nonlinearity can be enhanced by an order of magnitude compared to the standard Ti:Sapphire cavity, allowing mode locking with an output coupler reflectivity as low as R=55% and record-low intra-cavity pulse intensity. Our results provide an important new possibility to control mode-locking in cavities with very low intra-cavity pulse intensity, such as semiconductor laser oscillators and high-repetition rate mode-locked lasers.**

***Keywords*—Titanium-sapphire lasers, Laser mode locking, Ultra-fast nonlinear optics.**

## I. Introduction

Passive Kerr lens mode-locking (ML) is a major concept in laser physics, used for generation of ultrashort pulses with femtosecond to picosecond duration [1], [2]. Passive ML in general relies on a saturable loss mechanism within the laser cavity that favors the generation of high intensity pulses. The common loss mechanism for generation of ultrashort pulses at the femtosecond scale is the optical Kerr nonlinearity, which is practically instantaneous. Combined with a special cavity configuration, Kerr nonlinearity can produce an effective ultra-fast saturable loss by self-focusing (and self-phase modulation) of the pulsed laser beam. This can enhance the transmission through an effective aperture, thereby preferring ML operation compared to CW [3]. Usually the intensity dependence of the refractive index is weak ($\sim 10^{-16} cm^2/W$), indicating that only pulses of high peak intensity will be affected. To harness the Kerr effect for ML, the cavity is designed such that an extra Kerr lens reduces the intra-cavity loss for pulses, either by focusing through an additional physical aperture [4] after the Kerr lens, or by pushing the cavity slightly beyond the spatial stability range [5], where the continuous wave (CW) suffers from diffraction losses. The added Kerr lens then re-stabilizes the cavity then for pulses and reduces the effective loss.

Generally, ML of Ti:Sapphire oscillators operates best with repetition rates in the 50-150MHz range. However, many applications would benefit from higher repetition rates, especially frequency-comb based measurements, where a large spacing between the comb teeth is desired (in the range of few-to-tens GHz) [6], [7], [8]. The major obstacles for Kerr-lens ML with such high repetition rates is the inevitable reduction of the intra-cavity pulse energy due to the reduced round-trip time. The Kerr mechanism therefore becomes less efficient at high repetition rates, eventually precluding ML all together. The standard method to combat this restriction is to maintain the pulse intensity at the Kerr lens in spite of the reduction of the pulse energy by tightening the intra-cavity focus on the crystal [9], [10], [11], enhancing the output coupler (OC) reflectivity and increasing the pump power. However this standard approach is limited, since while these actions increase the intra-cavity pulse intensity, they also provide better conditions for CW operation, reducing the ML robustness, and eventually spurring the laser to CW operation.

We present a different approach: Instead of preserving the pulse intensity by tightening the focus and lowering the OC loss, we enhance the nonlinearity inside the cavity [12], [13], [14], [15] to allow efficient ML, even with lower intra-cavity pulse intensity. Thus, the threshold for ML operation [16] can be reduced to allow low-energy pulses to win over CW in the mode-competition. In the past, we used enhanced nonlinearity to demonstrate reduction of the ML threshold below the CW threshold [16]. Here we harness the enhanced nonlinearity to specifically target the intra-cavity pulse intensity and explore its limits and effects.

## II. Experimental setup

Our cavity configuration (Fig.1) was a slightly modified version of the standard X-folded four-mirror resonator for solid-state Kerr-lens ML oscillators. The gain medium was located at a cavity focal point, and a lens-based telescope of unit magnification formed an additional focus in the cavity, where a window with enhanced Kerr lensing was located to control the intra-cavity nonlinearity independent of the cavity gain. To compensate for the intra-cavity group delay dispersion (GDD), a combination of chirped mirrors and a prism-pair was used. The chirped mirrors compensated for the static cavity elements: the gain medium (3mm Ti:Sapphire) and the telescope lenses (7.6mm UV Fused Silica), while the prism-pair compensated for the additional Kerr window and allowed continuous GDD tuning. In all, the negative GDD was tunable up to -530 fs$^2$, equivalent to 3mm of highly dispersive SF6 glass at 850nm.

For the additional nonlinear window we used several types of glass at normal incidence (all windows were coated for anti-reflection) with various nonlinear coefficients in the range of $2 - 20 \times 10^{-16}$ cm$^2$/W, and different thicknesses (1mm and

The authors are with the Department of Physics and BINA Center of nano-technology, Bar-Ilan University, Ramat-Gan 52900, Israel (e-mail: Avi.Peer@biu.ac.il ; mallachi86@gmail.com). This work was supported by the Israel Science Foundation (ISF) (807/09, 46/14).

This article has been accepted for publication in a future issue of this journal, but has not been fully edited. Content may change prior to final publication. Citation information: DOI 10.1109/JQE.2017.2670544, IEEE Journal of Quantum Electronics



2mm). For low and moderate nonlinear enhancement, we used windows of BK7 glass, with a Kerr nonlinearity of $n_2^{BK7} = 3.5 \times 10^{-16}$ cm$^2$/W, which is similar to the nonlinearity of the sapphire crystal, whereas for significant nonlinear enhancement we used windows of SF11 glass ($n_2^{SF11} = 13 \times 10^{-16}$ cm$^2$/W) and SF6 ( $n_2^{SF6} = 22 \times 10^{-16}$ cm$^2$/W) [17], [18], whose nonlinear coefficient is 4-7 time larger than that of the sapphire crystal.

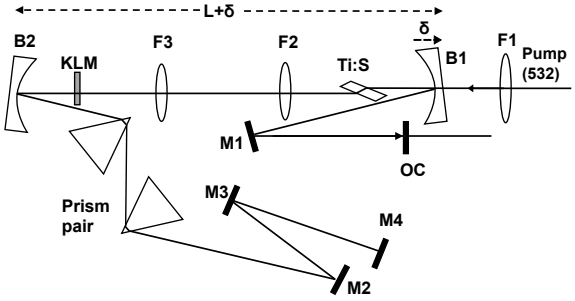


Fig. 1. Cavity configuration. The gain medium was a 3mm long Brewster-cut TiS crystal with 0.25% wt doping and pump absorption coefficient of $\alpha_{\lambda=532} = 4.6cm^{-1}$. The focal length of the curved mirrors (B1,B2) was $f = 7.5cm$. All of the intra-cavity mirrors (B1,B2,M1-M4) were chirped, introducing a total negative GDD of -450 fs$^2$, The telescope lenses (F2,F3) had a focal length of $f = 10cm$. The long cavity arm $L_2$ (between B2-M4) was 100cm long and contained a Brewster prism-pair of BK7 glass, and the short cavity arm $L_1$ (between B1-OC) was 50 cm long and contained the OC as the end mirror. The total cavity length was 2m (75MHz repetition). During the experiment we scanned the position of the curved mirror B1 ($\delta$) and optimized the Ti:S crystal and the pump lens position for each point to maximum CW power. The position of the KLM glass was set to the minimal ML threshold and the prisms were set to the broadest achievable spectrum.

## III. Experimental procedure and results

Our ML concept relied on the "Virtual Hard Aperture" technique [19], where by pushing the laser slightly beyond the spatial stability limit, diffraction losses are introduced for CW operation, while for intense pulses, the additional Kerr lens re-stabilizes the cavity and reduces the diffraction loss. Hence, the distance between the two curved mirrors was set to $L = 2f_{mirror} + 4f_{lens} + \delta_1$, where the offset from perfect telescope is $\delta_1 = f_{mirror}^2/(L_2 - f_{mirror})$, which marks the stability limit for the "plane-point" spatial mode (planar beam on the OC, and near point image of the cavity focus on the HR M4). $L_2$ is the length of the long arm of the cavity, defined as the distance between the curved mirror B2 and the HR end mirror M4. This configuration is our starting point for the characterization of ML: From $\delta_1$ , we scanned the position of the curved mirror B1 further into the unstable region $(\delta > \delta_1)$ , and measured the pump threshold for ML (defined as the minimum pump power that enables initiation of pulsed operation), the output power for ML and the output power for CW (at this pump threshold). The ratio between the CW power and the ML power at the ML threshold defines a quality parameter for ML:

$$\gamma = \frac{P_{CW}}{P_{ML}}, \tag{1}$$

which quantifies the advantage of ML operation over CW in the "mode-competition" between them [16]. This parameter relates to the difference in overall loss between the CW and the ML operation. When ML is preferable, $\gamma < 1$ while for $\gamma > 1$ the CW operation is favorable. Note that due to the soliton nature of ML the pulsed output power at the ML threshold is not zero, but rather the soliton-maintaining power. For a given mode-locking point at $(\delta > \delta_1)$, further increasing of the pump above the ML threshold will increase the CW output power, while the ML output power will remain approximately the same, as illustrated in Fig. 2, and as expected from a soliton pulse which indicates that pulsed operation is favorable only in a narrow range of pump power levels.

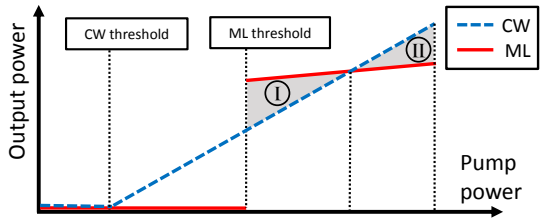


Fig. 2. ML and CW output power vs pump power. ML in the soliton regime is stable within a small parameter range (marked I), where the ML power is higher than the CW power. Increasing the pump power beyond the "trend-point" (marked II) favors again CW, and ML breaks either to CW or to multiple pulses.

Experimentally, the ML threshold was determined by locking at a high pump power (and high CW power) and slowly reducing the pump power while breaking ML and attempting to relock at every new pump level. The lowest pump power that allowed ML operation was the threshold for ML.

To optimize ML with low intra-cavity power, we explored the interplay between the OC reflectivity and the Kerr nonlinearity of the added window. For every OC-Kerr combination, we scanned the curved mirror B1 location to search for the optimal ML performance, and measured the reduction in intra-cavity pulse-energy that was enabled by the enhanced nonlinearity. We started the experiment with a standard OC of relatively high reflectivity (R=95%), where the intra-cavity power is sufficient for ML based on the sapphire nonlinearity alone without an additional nonlinearity. By measuring the ML quality factor $\gamma$ as a function of mirror position $\delta$ , we estimated the nonlinearity efficacy at different locations within the unstable range (see Fig. 3 for example). The general tendency of the graph is that the ML quality improves ($\gamma$ reduces) as we move further into the unstable region, (due to effective Kerr lensing for ML and increased diffraction losses for CW) up to an optimal location ($\delta_{opt}$), where the minimal $\gamma$ is obtained, marking the optimal ML-to-CW discrimination for the given OC-Kerr window combination. The parameters that indicate the ML quality are the minimum value $\gamma_{opt}$, the minimum location $\delta_{opt}$ , and the width of the dip. For better ML performance, the dip should be wide, deep, and at a high $\delta_{opt}$ value (see Fig. 3 (a)), whereas poor ML performance is marked by a shallow dip at a $\delta_{opt}$ close to the stability limit $\delta_1$, as illustrated in Fig. 3 (b).

This article has been accepted for publication in a future issue of this journal, but has not been fully edited. Content may change prior to final publication. Citation information: DOI 10.1109/JQE.2017.2670544, IEEE Journal of Quantum Electronics



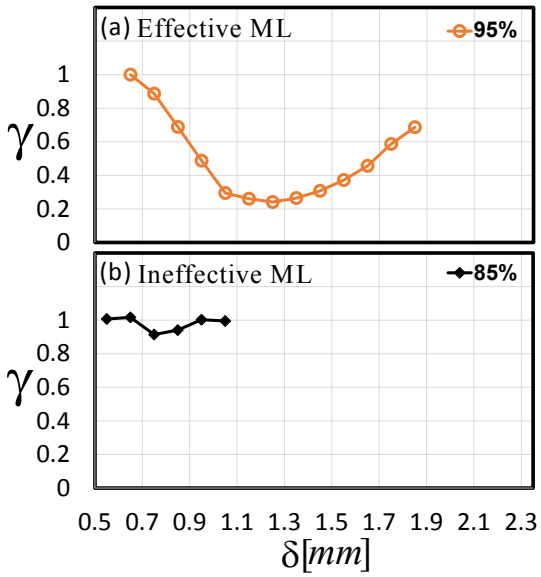


Fig. 3. Examples of ML quality scans. The position $\delta$ of the curved mirror B1 was measured with respect to $\delta_1$=6 mm which is the offset from perfect telescope for the plane-point stability limit. (a) cavity with 95% OC reflectivity, where ML is efficient, compared to (b) a cavity with 85% OC reflectivity, where ML is marginal.

We first observed the performance of ML without an additional Kerr window for various OCs (see Fig. 4 (a)). As expected, for a lower OC reflectivity, $\gamma$ showed a shallower minimum, much closer to the stability limit. With an OC reflectivity of 85% , $\gamma$ remained close to unity throughout the $\delta$-scan and ML could no longer compete with CW. This OC-limit marked the need to enhance the cavity nonlinearity (Fig. 4 (b)). With enhanced nonlinearity, the reduction of the OC reflectivity could continue even further (Fig. 4 (c-d)) until the OC-limit was hit again, the nonlinearity was increased again, and so on.

The trend in Fig. 4 (a) is clear: As the OC reflectivity is decreased, the ML performance degrades until the intra-cavity intensity is barely-sufficient to maintain ML. Increasing the nonlinearity overcomes this barrier, as shown in Fig. 4 (b). Indeed, with an additional non-linear window, the ML quality improved again (similar to the higher OCs before), allowing the OC reflectivity to be lowered further, as shown in Fig. 4 (c) The lowest OC reflectivity we could reach was R=55% with the strongest non-linearity available, (2mm of SF6 glass).

Let us now examine the measured intra-cavity peak intensity and pulse energy of selected configurations. Fig. 5 presents the intra-cavity pulse energy along the scan, when using 2mm SF6 glass (bottom graph) compared to a configuration with no nonlinear enhancement (Ti:Sapphire only), and OCs of 95% (top) and 85% (middle). Fig. 5 clearly shows that by adding a Kerr window of 2mm of SF6 glass, the ML average intra-cavity pulse intensity was reduced by a factor of 20 (at least) compared to the 95% OC, indicating that the cavity repetition rate could potentially be increased by a factor of 20, using enhanced nonlinearity with the same OC (95%) and with no

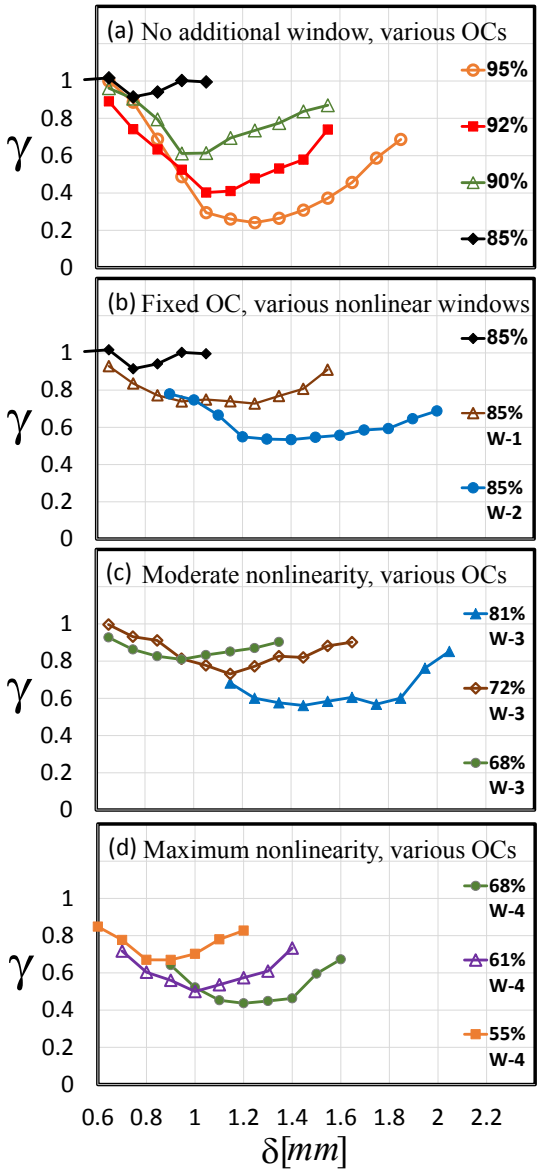


Fig. 4. Results: ML quality scans for various nonlinear enhancements with different OCs. The origin of the x-axis is x = $\delta_1$ . The additional nonlinear windows are 2mm BK7(w-1), 1mm SF11 (w-2), 2mm SF11 (w-3), and 2mm SF6 (w-4). (a) Cavities with no additional nonlinearity (only the Ti:Sapphire) and various OCs. (b) Gradually enhanced nonlinearity at fixed OC (R=85%). (c+d) reduction of the OCs reflectivity with enhanced nonlinearity.

change of other cavity parameters (focusing, gain, etc.).

The intra-cavity peak intensity and power of the ML laser with the R=55% OC reflectivity can be compared to that of the highest repetition rate Ti:Sapphire ML laser configurations published so far [9], [10], [11]. Near the working point, $\delta$=0.6mm , we achieved record-low intra-cavity average power of 0.32W [20], intra-cavity pulse energy of 3.2nJ and intra-cavity pulse intensity of 18 GW/cm$^2$, an improvement of factor >3 compared to the best peak intensity reported of 60 GW/cm$^2$, and pulse energy of 5.3nJ, from [9], [10], and

TABLE I. EXTENDED PERFORMANCE DATA FOR VARIOUS CAVITIES

| OC | Additional nonlinearity (mm) | ML / CW threshold(1) (W) | $\delta_{opt}$ (mm) | ML / CW output power (mW) | $\gamma_{min}$ quality parameret | Pulse duration(2) (fs) | beam area(3) $(\mu m)^2$ | Intra-cavity peak Intensity (GW/cm$^2$) |
|---|---|---|---|---|---|---|---|---|
| 95% | – – – | 2.7 / 2.4 | 1.25 | 199 / 48 | 0.24 | 16 | 785 | 417 |
| 92% | – – – | 2.9 / 2.5 | 1.15 | 268 / 110 | 0.41 | 17 | 664 | 373 |
| 88% | – – – | 2.8 / 2.2 | 0.85 | 324 / 222 | 0.68 | 19 | 622 | 308 |
| 85% | 2(BK7) | 2.8 / 1.9 | 0.75 | 315 / 288 | 0.91 | 21 | 424 | 298 |
| 85% | 3(BK7) | 3.0 / 2.5 | 1.15 | 300 / 222 | 0.74 | 25 | 558 | 180 |
| 85% | 1(SF11) | 3.2 / 2.7 | 1.3 | 340 / 227 | 0.66 | 25 | 534 | 206 |
| 85% | 2(SF11) | 3.2 / 3.0 | 0.7 | 281 / 150 | 0.53 | 27 | 543 | 156 |
| 81% | 2(SF11) | 3.7 / 3.5 | 1.75 | 235 / 133 | 0.56 | 28 | 550 | 98 |
| 72% | 2(SF11) | 3.6 / 3.2 | 1.15 | 238 / 174 | 0.73 | 29 | 506 | 66 |
| 68% | 2(SF6) | 3.7 / 3.4 | 1.2 | 268 / 117 | 0.43 | 30 | 562 | 56 |
| 61% | 2(SF6) | 4.2 / 3.9 | 1.0 | 236 / 118 | 0.5 | 32 | 532 | 38 |
| 55% | 2(SF6) | 4.4 / 4.0 | 0.8 | 212 / 142 | 0.67 | 46 | 528 | 20 |
| 55% | 2(SF6) | 3.8 / 3.4 | 0.6 | 145 / 123 | 0.84 | 45 | 394 | 18 |

(1) Both CW threshold and ML threshold were evaluated at the gain crystal.
(2) The pulse duration was estimated from the measured output spectrum assuming a transform limited pulse.
(3) Beam area is estimated at the gain crystal by measuring the ML beam at the output and propagation back to the gain crystal.

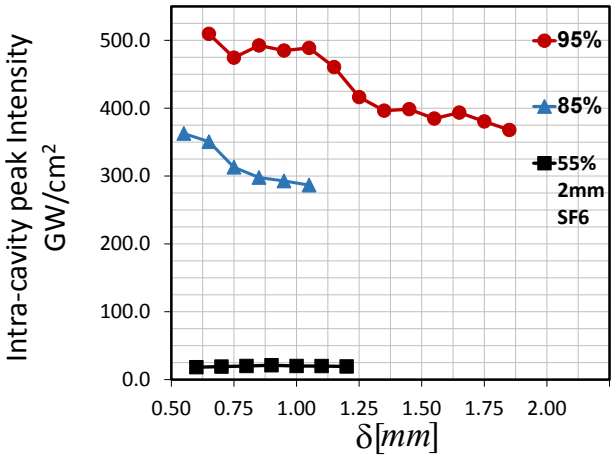


Fig. 5. ML average intra-cavity pulse energy across the $\delta$-scan with various OCs. The top curve denotes the cavity with 95% OC reflectivity without nonlinearity enhancement, the middle curve denotes 85% OC reflectivity without nonlinearity enhancement, and the lowest curve denotes the lowest OC with an additional nonlinear window of 2mm SF6.

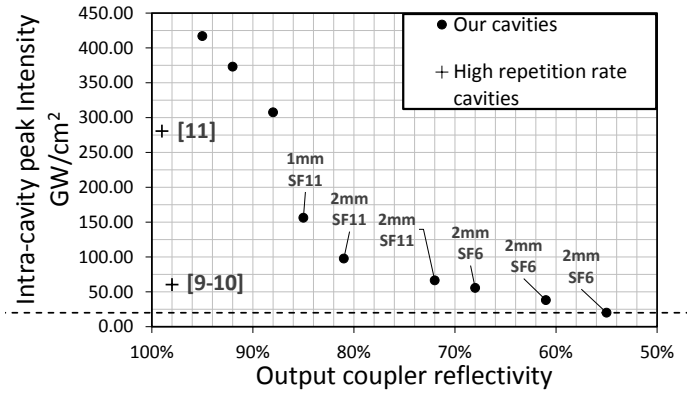


Fig. 6. Intra-cavity peak intensity at the "sweet point" ($\delta_{opt}$ of the ML quality factor, $\gamma_{min}$) for various nonlinear windows as a function of the OC reflectivity. The round markers denote different configurations of our system. The '+' sign represent references [9], [10], [11]. The peak intensity of [9], [10] was estimated based of the reported pulse duration and the pump focusing lens. To estimate the focal waist, we assumed a pump beam diameter at the pump-lens of 2.25 mm, the common beam diameter for standard pump lasers at 532nm (Verdi, Millennia, Sprout, etc...). for full characterization of the "sweet point" see chapter four (Discussion - temporal/spectral performance).

270 GW/cm$^2$, and 15nJ pulse from [11]. Note that this record result was achieved with a very mild focus in the crystal, whereas previously published configurations used much tighter focusing. Clearly, tighter focusing in our configuration could help as well to achieve ML with even lower pulse-energies. Finally, Fig. 6 summarizes the comparison of intra-cavity peak intensity in our experiment to previously published results.

## IV. DISCUSSION - TEMPORAL/SPECTRAL PERFORMANCE

To give a better picture of the laser performance of our cavity configuration, we characterized points where optimal performance was observed for all the cavities that were mentioned in Fig. 6. Table 1 presents this data of each OC-Kerr configuration in terms of ML/CW threshold, ML/CW output power, $\gamma$, pulse duration, modal beam area at the focus and peak-intensity. Note the trend of the pulse duration that slowly increases from $\sim$ 15fs to $\sim$ 45fs as the output coupler is reduced from 95% to 55%. While this is a well-known effect of reduction the OC, we cannot pinpoint the source of the pulse elongation since several additional relevant parameters were changed between these configuration.

## V. CONCLUSION AND OUTLOOK

We explored the usage of an additional intra-cavity Kerr medium to reduce the intra-cavity peak intensity necessary to maintain mode-locking in Ti:Sapphire oscillators. We achieved ML with low intra-cavity pulse intensity of 18 GW/cm$^2$ and average intra-cavity power of 340 mW by adding a Kerr window of 2mm SF6 glass. Our results clearly indicate that the intra-cavity intensity can be reduced by a factor of at least 15 (compared to a cavity without additional nonlinearity). Clearly, tighter focusing can reduce the necessary pulse energy

even further. The capability to operate with low intra-cavity intensity is important for ML configurations with low pulse energy, such as high repetition rate frequency combs or lasers with semiconductor based gain media. Our results provide a new approach for mode-locking, with new types of lasers.

## REFERENCES


[1] F. X. Kärtner, E. P. Ippen, and S. T. Cundiff, *Femtosecond optical frequency comb: principle, operation and applications*, ch. 2. Springer Science & Business Media, 2005.

[2] U. Keller, *Laser Physics and Applications. part 1*, ch. 2. Springer, 2007.

[3] E. P. Ippen, "Principles of passive mode locking," *Applied Physics B Laser and Optics*, vol. 58, pp. 159–170, mar 1994.

[4] H. Haus, J. Fujimoto, and E. Ippen, "Analytic theory of additive pulse and kerr lens mode locking," *IEEE Journal of Quantum Electronics*, vol. 28, no. 10, pp. 2086–2096, 1992.

[5] C. Spielmann, P. Curley, T. Brabec, and F. Krausz, "Ultrabroadband femtosecond lasers," *IEEE Journal of Quantum Electronics*, vol. 30, pp. 1100–1114, apr 1994.

[6] T. Ideguchi, S. Holzner, B. Bernhardt, G. Guelachvili, N. Picqué, and T. W. Hnsch, "Coherent raman spectro-imaging with laser frequency combs," *Nature*, vol. 502, pp. 355–358, oct 2013.

[7] T. Ideguchi, A. Poisson, G. Guelachvili, N. Picqué, and T. W. Hnsch, "Adaptive real-time dual-comb spectroscopy," *Nature Communications*, vol. 5, feb 2014.

[8] R. J. Jones, T. Ido, T. Loftus, M. Boyd, A. Ludlow, K. Holman, M. Thorpe, K. Moll, and J. Ye, "Stabilized femtosecond lasers for precision frequency metrology and ultrafast science," *LASER PHYSICS-LAWRENCE-*, vol. 15, no. 7, p. 1010, 2005.

[9] D. C. Heinecke, A. Bartels, and S. A. Diddams, "Offset frequency dynamics and phase noise properties of a self-referenced 10 GHz ti:sapphire frequency comb," *Opt. Express*, vol. 19, p. 18440, sep 2011.

[10] A. Bartels, D. Heinecke, and S. A. Diddams, "10-GHz self-referenced optical frequency comb," *Science*, vol. 326, pp. 681–681, oct 2009.

[11] T. M. Fortier, A. Bartels, and S. A. Diddams, "Octave-spanning ti:sapphire laser with a repetition rate greater 1-GHz for optical frequency measurements and comparisons," *Optics Letters*, vol. 31, p. 1011, apr 2006.

[12] J. Herrmann, "Theory of kerr-lens mode locking: role of self-focusing and radially varying gain," *Journal of the Optical Society of America B*, vol. 11, p. 498, mar 1994.

[13] R. Ell, U. Morgner, F. X. Krtner, J. G. Fujimoto, E. P. Ippen, V. Scheuer, G. Angelow, T. Tschudi, M. J. Lederer, A. Boiko, and B. Luther-Davies, "Generation of 5-fs pulses and octave-spanning spectra directly from a ti:sapphire laser," *Optics Letters*, vol. 26, p. 373, mar 2001.

[14] G. W. Pearson, C. Radzewicz, and J. S. Krasinski, "Analysis of self-focusing mode-locked lasers with additional highly nonlinear self-focusing elements," *Optics Communications*, vol. 94, pp. 221–226, nov 1992.

[15] X. Han and H. Zeng, "Kerr-lens mode-locked ti:sapphire laser with an additional intracavity nonlinear medium," *Opt. Express*, vol. 16, p. 18875, oct 2008.

[16] S. Yefet and A. Pe'er, "Mode locking with enhanced nonlinearity - a detailed study," *Opt. Express*, vol. 21, p. 19040, aug 2013.

[17] J. E. Aber, M. C. Newstein, and B. A. Garetz, "Femtosecond optical kerr effect measurements in silicate glasses," *Journal of the Optical Society of America B*, vol. 17, p. 120, jan 2000.

[18] R. Sutherland, D. McLean, and S. Kirkpatrick, *Handbook of Nonlinear Optics*. CRC Press, apr 2003.

[19] S. Yefet and A. Pe'er, "A review of cavity design for kerr lens mode-locked solid-state lasers," *Applied Sciences*, vol. 3, pp. 694–724, dec 2013.

[20] A. M. Kowalevicz, T. R. Schibli, F. X. Krtner, and J. G. Fujimoto, "Ultralow-threshold kerr-lens mode-locked ti:al_2o_3 laser," *Optics Letters*, vol. 27, p. 2037, nov 2002.


**Avi Pe'er** Avi Pe'er is a professor of Physics at Bar-Ilan University, Israel. He leads an experimental group focused on precision measurement using frequency comb sources, laser physics and quantum optics. Avi received his BSc in Physics and Computer Science from Tel Aviv University in 1996, and his PhD in Physics from the Weizmann Institute of Science in 2005. Between 2005-2008 Avi was a post-doctoral fellow with Jun Ye at JILA, University of Colorado, specializing on precision light-matter interaction using the frequency comb.

**Mallachi Elia Meller** received the B.S. degrees in applied physics from Bar Ilan University, Israel, in 2015. He is currently a PhD student in the Physics Department, Bar Ilan, Israel.

**Shai Yefet** Shai Yefet received his Ph.D. from Bar-Ilan university in 2013 under the supervision of Prof. Avi Pe'er, specializing in mode loked lasers and ultrafast phenomena. Currently, Shai is developing lasers for medical devices in in the private sector.